Welding thermal cycle impact on the microstructure and mechanical properties of thermo-mechanical control process steels

Anatoliy Zavdoveev, Valeriy Poznyakov, Thierry Baudin, Mark Heaton, Hyoung Seop Kim, Philippe Acquier, Mykola Skory, Massimo Rogante, Anatoliy Denisenko

Welding thermal cycle impact on the microstructure and mechanical properties of TMCP steels

Anatoliy Zavdoveev, Valeriy Poznyakov, Thierry Baudin, Mark Heaton, Hyoung Kim, Philippe Acquier, Mykola Skory, Massimo Rogante, Anatoliy Denisenko

Welding Thermal Cycle Impact on the Microstructure and Mechanical Properties of Thermo–Mechanical Control Process Steels

Anatoliy Zavdoveev,* *Valeriy Poznyakov*, *Thierry Baudin*, *Mark Heaton*, *Hyoung Seop Kim*, *Philippe Acquier*, *Mykola Skory*, *Massimo Rogante*, and *Anatoliy Denisenko*

Steels obtained by the thermo–mechanical control process (TMCP) possess a higher level of strength than conventional normalized steels due to the fine-grained microstructures generated during TMCP. Such enhancement opens ways to decrease metal construction weight. At the same time, TMCP steels have less thermal stability, in connection with a lot of factors affecting and governing grain growth during the heating of TMCP steels. Herein, the effects of the welding thermal cycle (WTC) on the structure and properties of TMCP steels of ferritic–perlite (S460M) and bainitic (alform 620M) types are systematically investigated.

1. Introduction

In industry, developing steels with improved mechanical characteristics (increased level of strength) uses two approaches. The first one consists of applying alloying elements, i.e., increased strength of steel.[1] This method, nevertheless, leads to a significant increase in the price of manufactured rods. An alternative path for the alloying procedure is the thermo–mechanical control process (TMCP).[2–7] High-strength low-alloy (HSLA) steels obtained by controlled rolling with subsequent accelerated cooling are widely represented in the metal market. They are being introduced in machine building, metallurgy, mining, and processing industries.[8] The application of high-strength steels gives the opportunity to reduce the overall weight by up to 80% compared with steels of 300 MPa strength. Due to the high mechanical properties, this allows the creating of lightweight welded metal structures. The steel, micro-alloyed by niobium and vanadium, has high mechanical properties. Such material has a predominantly bainitic structure.[4,9,10] The addition of niobium, vanadium, and titanium contributes to the reaustenization of the metal by preventing the growth of austenitic grain. Dispersion hardening is effectively controlled by the vanadium content.[11–13]

The modern construction and energy industries have put force on new metalware demands in their steel intensity and increasing reliability.[2,3,14–17] This effect could be reached by adopting new high-strength TMCP steels with yield stress more than 390 MPa. The application of welding technologies for high-strength steels obtained by the TMCP methods is based only on the recommendations of the metal and welding materials' manufacturers as well as the carbon equivalent. The resulting properties can be lost as a consequence of softening during the operations associated with heating of steel. It is known that the microstructure and mechanical properties of metal can significantly change under the influence of welding thermal cycles (WTC).[4] To design the sound technology for structure manufacturing, it is essential to know the impact of rapid heating/cooling on the mechanical properties of welded

Dr. A. Zavdoveev, Prof. V. Poznyakov, Dr. A. Denisenko
Paton Electric Welding Institute of NAS
Bozhenko n. 11, Kiev 03680, Ukraine
E-mail: zavdoveev@paton.kiev.ua

Prof. T. Baudin
CNRS
Institut de chimie moléculaire et des matériaux d'Orsay
Université Paris-Saclay
Orsay 91405, France

Dr. M. Heaton
ANT
Advanced Nano Technology
Nandor Rd, Park West business park, Dublin, Ireland

The ORCID identification number(s) for the author(s) of this article can be found under https://doi.org/10.1002/srin.202000645.

Prof. H. S. Kim
Department of Materials Science and Engineering
Pohang University of Science and Technology (POSTECH)
Pohang 37673, Korea

Dr. P. Acquier
AddUp FRANCE
5 rue bleue, ZI de Ladoux, Cébazat 63118, France

Dr. M. Skory
G. V. Kurdyumov Institute of Metal Physics of the NAS of Ukraine
NanoMedTech LLC
Kyiv, Ukraine

Dr. M. Rogante
Rogante Engineering Office
Contrada San Michele n.61, Civitanova Marche 62012, Italy

DOI: 10.1002/srin.202000645

Q3 metals. As far as we know, weldability determines the creation of the sound joint with equal or close mechanical properties. Thus, during the first step of this research, the effects of WTCs on the properties and microstructures of the heat-affected zone (HAZ) metal of HSLA steels grade S460M and alform 620M microalloyed with niobium and vanadium have been investigated.

2. Experimental Section

The structural steels grade S460M and alform 620M having a thickness of 16 mm were selected for the experiments. The TMCP-hardened steels S460M (strength class 440 MPa) and alform 620M were manufactured according to the EN 10025-4: 2007 norm. The chemical compositions are shown in **Table 1**. For the criterion of WTCs, the cooling rate ($W_{6/5}$) in the temperature range of 600–500 °C of samples heated up to 1300 °C was chosen (interval of minimum equilibrium of austenite).

Based on the research results,[18,19] the cooling rates were determined at the temperature range in which the HAZ metal strength, ductility, and toughness indices decreased compared with the regulated requirements for welded joints. The change in the mechanical properties in relation to the HAZ metal cooling rate in the 600–500 °C temperature range ($W_{6/5}$) was studied with $120 \times 12 \times 12\,mm^3$ model samples, which were heat treated in accordance with WTC (**Figure 1**). The heat-treatment process was the following. The samples, crossed by current, were first heated to temperatures in the range 1200–1300 °C, which are typical for the coarse-grained HAZ of welded joints. The heating rate was in the range 150–170 °C s^{-1}, which corresponded to the conditions of metal heating in the zone of thermal influence during the arc-welding processes. The samples were held at such a temperature for ≈2 s, and then they were forcedly cooled. In the current study, the cooling rate $W_{6/5}$ varied from 3 to 25 °C s^{-1}.

Table 1. a) The as-received steel S460M and b) alform 620M: chemical composition, wt%.

	C	Si	Mn	P	[S]	Al	Cr	Mo	Ni	V	[Nb]	Ti
a)	0.15	0.23	1.3	0.017	0.01	0.025	0.09	–	0.02	0.01	0.05	–
b)	0.08	0.37	2.0	0.005	0.01	0.027	0.38	0.21	0.02	0.01	0.043	0.017

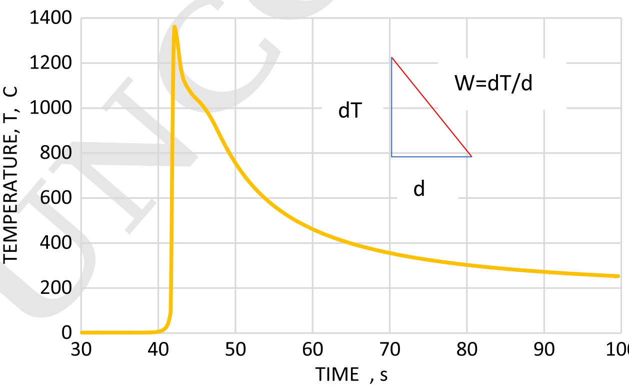

Figure 1. WTC (Cooling rate W is defined as $dT/d\tau$).

The mechanical properties, namely the yield strength (YS), ultimate tensile strength (UTS), plasticity (δ: uniform elongation, ψ: area reduction), and the impact strength (KCV), were evaluated. For a static tensile test of the steel, cylindrical samples with a 6 mm diameter of the working part were mechanically manufactured according to ASTM E8 standards. The tests were conducted at ambient temperature with a strain rate of $3 \times 10^{-5}\,s^{-1}$. For the impact strength determination, Charpy impact tests were conducted at the temperatures of +20, −20, and −40 °C ($10 \times 10 \times 55\,mm^3$ with V-shaped notch, according to the ASTM A370 norm).

Several methods were used for microstructure analysis: microhardness measurements, scanning electron microscopy (SEM), and electron backscatter diffraction (EBSD), and Oxford Instruments. The preparation of the metallographic specimens for microstructural studies was conducted according to standard methods using grinding papers of different roughnesses. Finishing polishing was conducted on a diamond suspension with a polishing particle size of 1 μm. For the finishing stage, a silica-colloidal solution of 0.04 μm was applied for polishing. To reveal and identify the microstructure morphology of the specimen, etching with a 4% solution of HNO_3 in alcohol was conducted. The exposure time of these specimens was 4 s, followed by washing and drying. The crystallographic orientation of the crystallites was determined using the EBSD technique. An electron scanning microscope Tescan Mira 3 LMU equipped with a Nordlys detector and HKL Channel 5 software were used for the EBSD analysis of structural changes. The following procedure was applied: the magnification of (×600–700) was used, whereas the scanning area was $150 \times 100\,\mu m^2$, the scanning step was 0.5 μm (at least five measuring points per grain), binning 4×4. The degree of indication was at least 80%.

3. Results and Discussion

The microstructure and mechanical properties of the as-received metal are the following: steel grade S460M: ferritic–pearlitic with strength level 460 MPa; steel grade alform 620M, bainitic with strength level 620 MPa. Due to special rolling and controlled cooling in the temperature range of 900–700 °C (TMCP) in S460M steel, a ferrite–pearlite, banded structure with a Vickers hardness of 195 HV was formed (see **Figure 2**a). In comparison, alform 620M steel possesses a bainitic (mostly lower bainitic—90%) structure (Figure 2b) with a grain size of about 40 μm and a hardness of 280 HV. The difference in structure type is determined by the chemical composition of studied steels. The presence of Mo in alform 620M steel shifts the bainitic region to the right on the continuous cooling temperature (CCT) diagram. This leads to the preferable formation of bainitic during decomposition of the overcooled austenite, even at a low cooling rate. Instead of this, the CCT diagram for S460M steel shows ferritic–pearlitic regions first and then at the increased cooling rate bainitic.[20]

Let us note that, based on the analysis of the microscopy images, it is impossible to determine the rolled strips, which must be present, taking into account the obtaining method of the aforementioned steel alform 620M (**Figure 3**). In this case, there is a structure of granular bainite without signs of rolling.

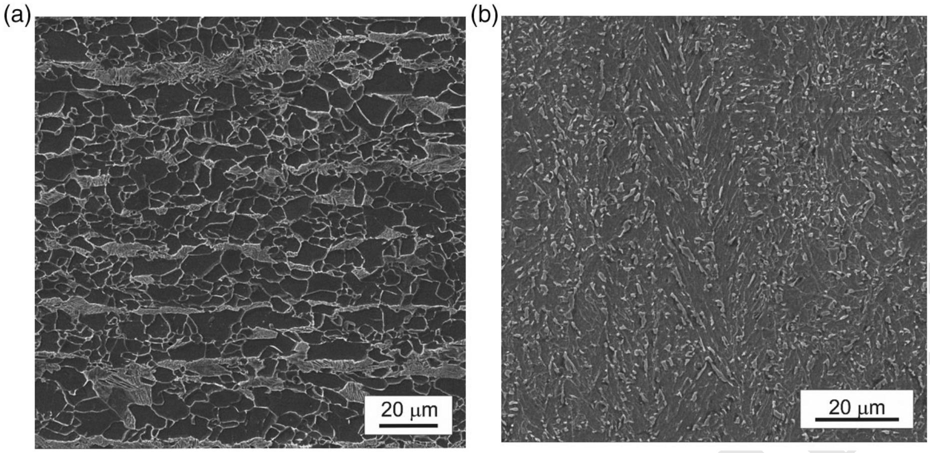

Figure 2. SEM micrographs of a) S460M and b) alform 620M steel.

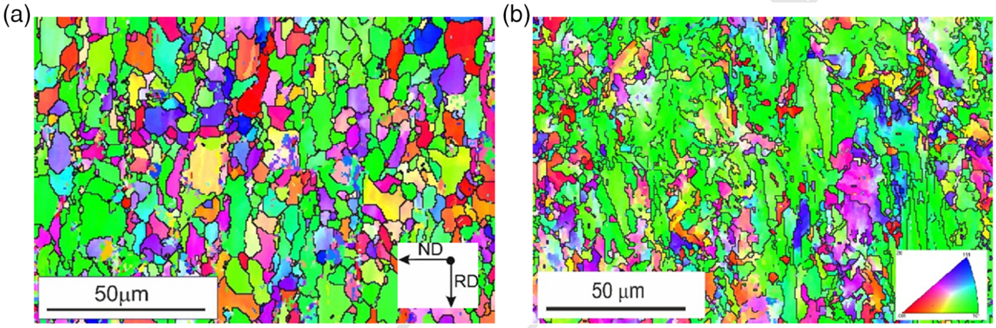

Figure 3. The EBSD orientation map of the a) S460M and b) alform 620M steel. Initial state. IPF, crystallographic direction // RD.

A measurement of the crystallographic orientations of the grains, therefore, was carried out using EBSD. In Figure 3, a map of the grain orientation distribution is shown.

The coloured areas correspond to grains and the black lines to the grain boundaries (misorientation angle > 15°). The data show that the overwhelming number of grains are green in colour, which corresponds to the {101} planes. The analysis of the texture ideal orientation EBSD maps (**Figure 4**a,b) has shown that for <101>//RD components, content is equal to 50% for S460M steel and 70% for alform 620M steel. It is known from the theory of crystallography that slip is most actively developed precisely in the {101} planes for body-centred cubic (bcc) crystals. The pole figures (Figure 4c,d) for this structure confirm the presence of {110}<111> texture; taking into account the information on the delivery status of the investigated high-strength steels, it can be argued that it corresponds to the rolling texture. This is important in this case, as the textured samples are susceptible to heating influence as texture is associated with deformation (here, rolling).

The dependencies characterizing the changes in the strength and ductility parameters in the simulated metal of the HAZ of S460M and alform 620M steels under the influence of WTC are shown in **Figure 5** and **6**.

The results indicate that with the change in the cooling rate from 3 to 25 °C s^{-1} in the temperature range 600–500 °C ($W_{6/5}$), the strength of the HAZ metal for S460M steel is increased in comparison with the initial state, namely, YS from 490 to 810 MPa and UTS from 600 to 1000 MPa. At the same time, the plastic properties of the simulated HAZ metal decrease in comparison with the initial state. This is especially true concerning the indices of the relative reduction psi, which is reduced 2.5 times, whereas the relative elongation is reduced only by 15%–20%.

In turn, the dependencies characterizing changes in the strength and ductility indices in the simulated HAZ metal of the alform 620M steel under the influence of the WTC are shown in Figure 5. The results of the conducted studies indicate that, with a cooling rate in the temperature range of 600–500 °C $W_{6/5} = 3$ °C s^{-1}, and the yield stress of the HAZ metal is lower than the initial state, namely decreases from 667 to 553 MPa. With a $W_{6/5}$ increase to 12 °C s^{-1}, the YS increases to 580 MPa and 585 MPa at $W_{6/5} = 25$ °C s^{-1}. The UTS decreases slightly to 723 MPa at $W_{6/5} = 3$ °C s^{-1} and then it increases to 790 MPa at $W_{6/5} = 25$ °C s^{-1}. At the same time, the plastic properties of the simulated HAZ metal do not change significantly as compared with the initial state (the changes do not exceed 5%–10%).

In the impact bending tests of the samples with a V-shaped notch, the impact strength of the S460M steel HAZ metal decreases with respect to the base metal (see Figure 6). The most significant decrease in the KCV values is 4–9 times in samples that cooled at the rate $W_{6/5} = 3$ °C s^{-1} (from 111 to 33 J cm^{-2} at the test temperature of +20 °C, from 109 to 15 J cm^{-2} at the temperature of −20 °C, and from 95 to 10 J cm^{-2} at a temperature of −40 °C).

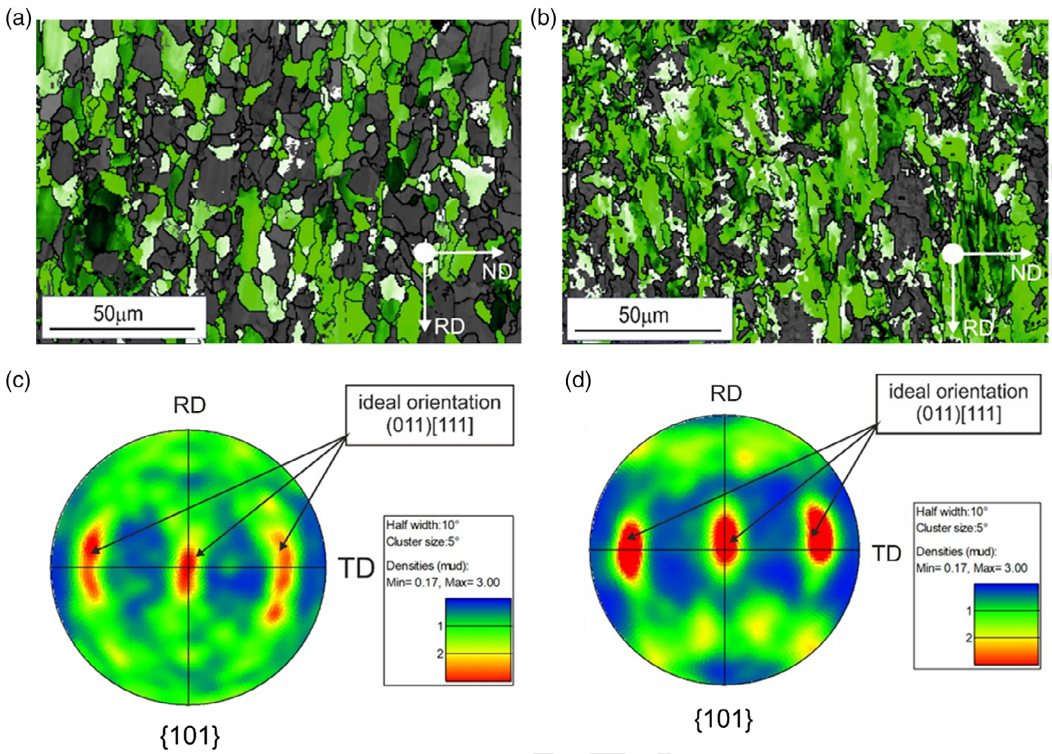

Figure 4. a,b) The texture ideal orientations EBSD map for <101>//RD components and c,d) pole figures where the ideal orientations for the rolling of bcc Fe are marked with arrows. a,c) Steel grade S460M and b,d) alform 620M steel. Initial state.

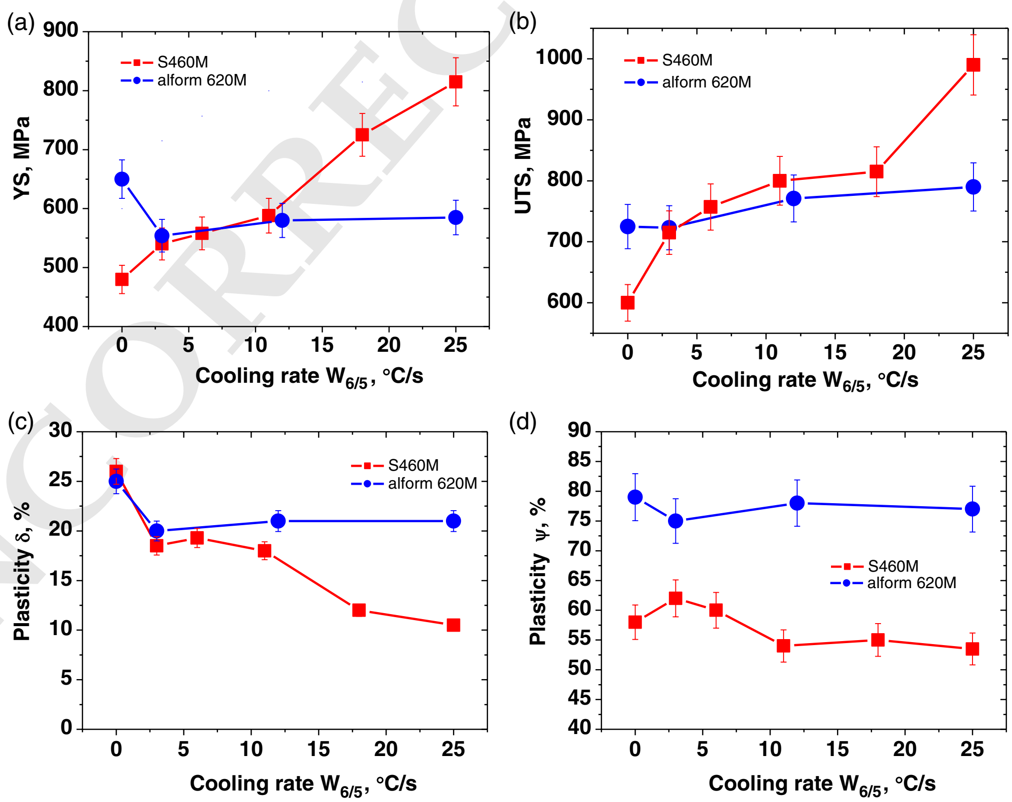

Figure 5. Mechanical properties of the S460M and alform 620M steel. a)YS, b) UTS, c) δ, and d) plasticity ψ.

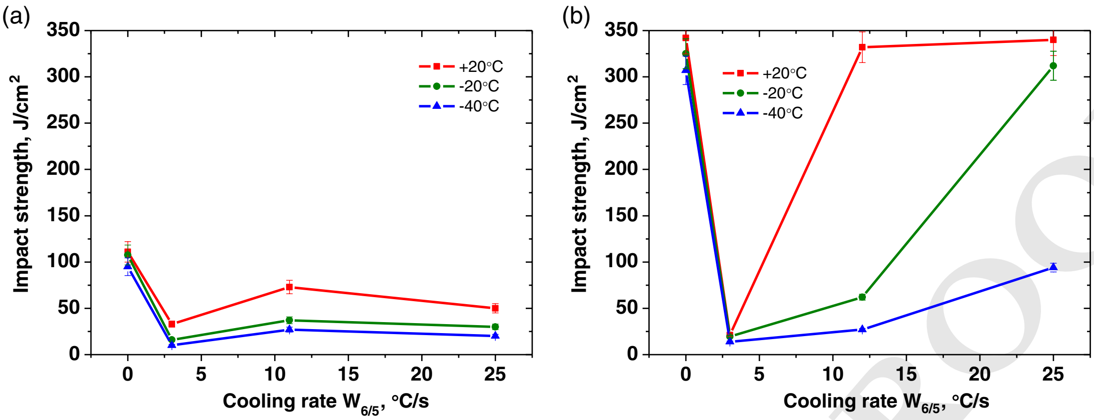

Figure 6. Impact strength of a) the S460M and b) alform 620M steel.

With an increase in the cooling rate to 10 °C s^{-1}, they increase to $KCV_{-40} = 27$ J cm^{-2}, then decrease somewhat, at $W_{6/5} = 25$ °C s^{-1}. The result is $KCV_{+20} = 50$ J cm^{-2}; $KCV_{-20} = 30$ J cm^{-2}; and $KCV_{-40} = 20$ J cm^{-2} (for comparison, the impact toughnesses of the S460M steel at test temperatures in the range from +20 to −40 °C are within 95–110 J cm^{-2}). The impact strength of the steel alform 620M significantly exceeds the standard values, and it is equal to 307 J cm^{-2}.

When testing the impact bending of the alform 620M steel specimens with a sharp V-shaped notch, it was established that the impact strength of the HAZ metal decreases in relation to the base metal (Figure 6). The most significant decrease in values is observed in the samples that cooled at a rate of $W_{6/5} = 3$ °C s^{-1} (from 341 to 21.2 J cm^{-2} at the test temperature of 20 °C, from 329 to 19.5 J cm^{-2} at a temperature of −20 °C, and from 307 to 14.3 J cm^{-2} at a temperature of −40 °C). With an increase in the cooling rate to 12 °C s^{-1}, they slightly increase for impact strength at negative temperatures and increase significantly for testing at room temperature: 332 J cm^{-2} (20 °C), 62 J cm^{-2} (−20 °C), and 27 J cm^{-2} (−40 °C). With an increase in cooling rate to 25 °C s^{-1}, they increase to the following values: 340 J cm^{-2} (20 °C), 312 J cm^{-2} (−20 °C), and 94 J cm^{-2} (−40 °C). Therefore, in terms of static strength, ductility, and toughness, the steel alform 620M can be considered promising from the point of view of its use for the equipment of the ore-dressing complex.

Such changes in the mechanical properties of the HAZ metal in S460M and alform 620M steels are due to different structural transformations in the range of the studied cooling rates. This is evidenced by the results of metallographic investigations. It has been revealed that for the S460M steel, the structure consisting of different morphological forms of ferrite and a small amount of perlite is formed in the HAZ metal at a cooling rate of $W_{6/5} = 3$ °C s^{-1}. The hardness of such a metal is 240 HV, and the bands of its microstructure, as observed before the thermal cycle, disappear completely. It has been found that for alform 620M steel in the HAZ metal, at a cooling rate of $W_{6/5} = 3$ °C s^{-1}, a microstructure is formed consisting of various morphological forms of lower and upper bainite, with the latter predominating and an average grains size of about 65 microns. The hardness of such metal is 220 HV.

An equiaxial ferrite–pearlite with a bainitic component is formed with a finely dispersed structure, with an increase in $W_{6/5}$ to 10 °C s^{-1} for S460M steel. The grain size, in this case, slightly increases to 15 μ and hardness is almost unchanged, although the strength indicators increase by ≈100 MPa. Due to a further increase in the cooling rate to $W_{6/5} = 25$ °C s^{-1} (**Figure 7**a) in the HAZ metal, a microstructure is formed consisting of a mixture of upper and lower bainite and a small amount of martensite and ferrite. Due to this fact, the hardness of the metal increases to 280 HV, which in turn leads to an increase in the indices of its static strength and drop in its plastic properties.

The studies of the WTC effect on the structure and properties of alform 620M steel have shown the following peculiarities.1) At the cooling rate of the simulated HAZ metal, $W_{6/5} = 3$ °C s^{-1} (characteristic of submerged arc welding processes). There is a significant decrease in the YS from 650 to 554 MPa and an impact strength to values not satisfying the requirements of Euronorm standards (i.e., less than 34 J cm^{-2}), due to a significant increase in the grain size of the structure obtained under such cooling conditions. 2) To increase the strength and impact strength, the cooling rate of the simulated HAZ metal should be increased up to $W_{6/5}$ to 25 °C s^{-1}. A fine-dispersed structure with a grain size of about 15–25 μm, at the same time, is formed in the HAZ metal, and the fracture surface of samples tested for impact bending has a brittle–viscous fracture-mixed structure.

4. Conclusions

The peculiarities of the WTC effect on the structure and mechanical properties of the TMCP steels of ferritic–pearlite (grade S460M) and bainite (grade alform 620M) classes are investigated. These steels have a difference in chemical composition content, i.e., bainitic steel possesses Mo and Cr. Such alloying provides higher thermal stability for alform 620M steel. These results provide knowledge for choosing optimal cooling rates.

It is proven that in the cooling rate range of $10 \le W_{6/5} \le 15$ °C s^{-1} related to the HAZ metal of the S460M steel model samples, the values of static strength, ductility, and impact toughness at the level of the base metal are retained. The cooling range of $10 \le W_{6/5} \le 25$ °C s^{-1} related to the HAZ

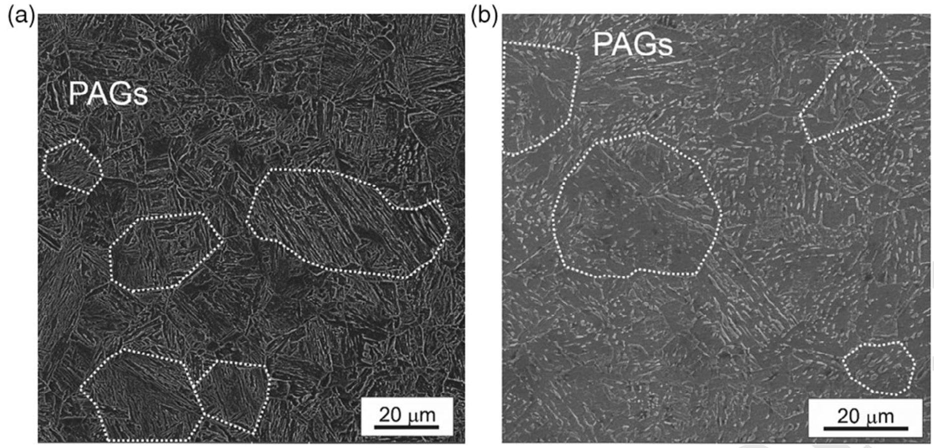

Figure 7. The SEM micrographs of a) the S460M and b) alform 620M steel HAZ metal. $W_{6/5} = 25\,^{\circ}\mathrm{C\,s^{-1}}$. Parent austenite grains (PAGs) are marked in white dotted lines.

metal of the alform 620M steel shows much more stable dependencies of mechanical properties.

Q4 Thus, steel S460M can be welded with the 10–15 $^{\circ}\mathrm{C\,s^{-1}}$ cooling rate heat input modes, whereas steel alform 620M can be welded in a much wider range. Submerged arc welding processes which are characterized by a low cooling rate 3–5 $^{\circ}\mathrm{C\,s^{-1}}$ can't be applied to any these steels.

Acknowledgements

The authors are grateful to Dr. S. Jdanov, Dr. A. Maksimenko, V.Kostin, and Dr. E. Berdnikova for their help in the experiments.

Conflict of Interest

The authors declare no conflict of interest.

Author Contributions

A.Z., T.B., M.R., and A.D. carried out the measurements. A.Z., T.B., V.P, and H.K. were involved in planning and supervised the work. A.Z., T.B., MR, P.A., and M.H. processed the experimental data, conducted the analysis, drafted the manuscript, and designed the figures. A.Z., T.B, F.B., and M.S. manufactured the samples and characterized them with EBSD and SEM. T.B., M.R., M.H., and P.A. aided in interpreting the results and worked on the manuscript. All authors discussed the results and commented on the manuscript.

Data Availability Statement

Research data are not shared.

Keywords

mechanical properties, microstructure, thermo–mechanical control processes, welding thermal cycles

Received: November 19, 2020
Revised: December 28, 2020
Published online:

[1] G. Larzabal, N. Isasti, J. Rodriguez-Ibabe, P. Uranga, *Metals* **2018**, *8*, 694. Q5
[2] J. Górka, in *Sci. Proc. X Int. Congr. Machines, Technol. Mater.*, **2013**, pp. 1313–0226. Q6
[3] C. H. Lee, H. S. Shin, K. T. Park, *J. Constr. Steel Res.* **2012**, *74*, 134.
[4] S. Lee, B. C. Kim, D. Kwon, *Metall. Trans. A.* **1992**, *23*, 2803.
[5] A. Zavdoveev, M. Rogante, V. Poznyakov, M. Heaton, P. Acquier, H. S. Kim, T. Baudin, V. Kostin, *Rep. Mech. Eng.* **2020**, *1*, 26.
[6] B. de Meester, *ISIJ Int.* **1997**, *37*, 537. Q7
[7] D. Porter, A. Laukkanen, P. Nevasmaa, K. Rahka, K. Wallin, *Int. J. Press. Vessel. Pip.* **2004**, *81*, 867.
[8] R. Song, D. Ponge, D. Raabe, J. G. Speer, D. K. Matlock, *Mater. Sci. Eng. A.* **2006**, *441*, 1.
[9] C. Fossaert, G. Rees, T. Maurickx, H. K. D. H. Bhadeshia, *Metall. Mater. Trans. A.* **1995**, *26*, 21.
[10] A. V. Nazarov, E. V. Yakushev, I. P. Shabalov, Y. D. Morozov, T. S. Kireeva, *Metallurgist.* **2014**, *57*, 911.
[11] O. Berdnikova, V. Pozniakov, A. Bernatskyi, T. Alekseienko, V. Sydorets, *Proc. Struct. Integr.* **2019**, 8916.
[12] Y. Sun, R. J. Hebert, M. Aindow, *Mater. Des.* **2018**, *156*, 429.
[13] J. Górka, *Arch. Metall. Mater.* **2015**, *60*, 1.
[14] A. Zavdoveev, V. Pozniakov, M. Rogante, S. Jdanov, A. Maksimenko, in *Int. Conf. "Mechanical Technologies and Structural Materials"*, **2017**.
[15] M. Alibeyki, H. Mirzadeh, M. Najafi, *Met. Mater.* **2018**, *56*, 297.
[16] A. Karmakar, M. Mandal, A. Mandal, M. Basiruddin Sk, S. Mukherjee, D. Chakrabarti, *Metall. Mater. Trans. A Phys. Metall. Mater. Sci.* **2016**, *47*, 268.
[17] A. V. Zavdoveev, S. L. Zhdanov, A. V. Maksimenko, V. D. Poznyakov, *Pat. Weld. J.* **2018**, *10*, 9.
[18] R. Demarque, E. P. dos Santos, R. S. Silva, J. A. de Castro, *Sci. Technol. Mater.* **2018**, *30*, 51.
[19] A. Zavdoveev, V. Pozniakov, M. Rogante, S. Jdanov, A. Maksimenko, *Mech. Technol. Struct. Mater.* **2017**, 163.
[20] G. M. Grigorenko, V. A. Kostin, T. A. Zuber, V. D. Poznyakov, *Pat. Weld. J.* **2017**, *10*, 2.